

Growth of Zinc Oxide Nanorods Using Various Seed Layer Annealing Temperatures and Substrate Materials

Kyung Ho Kim^{*}, Kazuomi Utashiro, Yoshio Abe, and Midori Kawamura

Department of Materials Science and Engineering, Kitami Institute of Technology, 165 Koen-cho, Kitami, Hokkaido 090-8507, Japan

*E-mail: khkim@mail.kitmai-it.ac.jp

Received: 10 December 2013 / Accepted: 4 January 2014 / Published: 2 February 2014

We fabricated zinc oxide (ZnO) nanorods (NRs) with ZnO seed layers by using the sol-gel solution method with various annealing temperatures on different substrate materials (silicon, glass, and fluorine doped tin oxide (FTO) coated glass). Within a certain range of seed annealing temperatures, the alignment and length of the NRs were significantly improved. However, the growth rate of the NRs was less affected by the substrate material at a fixed seed annealing temperature. From X-ray diffraction (XRD) measurements, the NRs grown on the silicon substrate exhibited better crystallinity than those grown on the glass and FTO coated glass substrates. During the growth process for the NRs, the self-attraction phenomenon occurred, which led to a decrease in the NR density and improved the alignment, resulting in a highly c-axis oriented ZnO NR growth on the substrate.

Keywords: ZnO, Nanorods, Seed layer, Annealing temperature, Substrate materials

1. INTRODUCTION

One-dimensional (1D) zinc oxide (ZnO) nanorods (NRs), which are direct wide band gap (3.37 eV) semiconductor with a large exciton binding energy (60 meV) at room temperature, have attracted considerable attention because of their application potential in a variety of fields, including chemical sensors, photodetectors, field-effect transistors (TFTs), piezoelectric generators, and solar cells [1-6]. The length and alignment of the ZnO NRs are vital parameters and play determining roles in their properties. These could be effectively improved by the seed layer, which reduces the lattice mismatch between the NRs and a substrate and leads to the growth of well-aligned NRs on the substrate [7,8].

In this study, the properties of ZnO NRs were investigated using different seed annealing temperatures (150–450 °C) prepared by the sol-gel solution method and NR growth times (3–12 h) on

various substrate materials (silicon, glass, and fluorine doped tin oxide (FTO) coated glass). Compared to other fabrication methods such as chemical vapor deposition (CVD), sputtering, pulsed laser deposition (PLD), and thermal evaporation, the sol-gel solution provides the advantages of an environmentally friendly process, simplicity, and low-cost fabrication, as well as a large-area process capability [9-11]. The seed annealing temperature was a critical factor in the growth of the ZnO NRs. At a certain seed annealing temperature, the lengths of the NRs grown on the various substrates showed no clear difference, whereas the crystallinity of the NRs grown on silicon was better than that of the NRs grown on the other substrates (glass and FTO). With increasing growth times, the length and density of the NRs increased and decreased, respectively, leading to well-aligned NRs on the substrate.

2. EXPERIMENTAL

2.1. Preparation of the ZnO seed layers

The ZnO seed layers were prepared using zinc acetate dehydrate [$\text{Zn}(\text{CH}_3\text{COOH})_2 \cdot 2\text{H}_2\text{O}$, Wako, 0.15 M] as a precursor dissolved in ethanol (Wako), 2-methoxyethanol (ME, Wako), and milli-Q solvents [12]. After stirring at 60 °C for 1 h, the sol was aged at room temperature for 24 h. The substrates (silicon, glass, and FTO coated glass) were subjected to a standard cleaning process using acetone, isopropyl alcohol, and deionized water for 10 min each, in a ultrasonic bath. After spin-coating the sol on the substrate, it was then annealed at different temperatures ranging from 150 °C to 450 °C for 30 min in the air ambient. The lowest annealing temperature of 150 °C was suitable for commercial plastic substrates and the highest annealing temperature of 450 °C was chosen because of its compatibility with annealing process of the FTO substrates in the dye-sensitized solar cells (DSSCs) [13,14]. The thickness of the ZnO layer was fixed at 20 nm.

2.2. Preparation of the ZnO NRs

The ZnO NRs were prepared using a hydrothermal method with an aqueous solution of zinc nitrate hexahydrate [$\text{Zn}(\text{NO}_3)_2 \cdot 6\text{H}_2\text{O}$, Sigma-Aldrich, 0.01 M] and hexamethylenetetramine (HMT) [$\text{C}_6\text{H}_{12}\text{N}_4$, Sigma-Aldrich, 0.01 M] [15]. The prepared seed layers were kept in the solution for 3–12 h at 90 °C. During the growth process, the entire solution was changed every 3 h. After that, the samples were washed several times using deionized water and dried at 120 °C for 10 min.

2.3. Characterization methods

The thickness of the seed layer was measured using variable-angle ellipsometry (MIZOJIRI, DVA-FL). The structural properties of the ZnO seed layer and NRs were examined using X-ray diffraction (XRD, Bruker, D8ADVANCE with Cu K α radiation, $\alpha = 1.5406 \text{ \AA}$) operating at a voltage of 40 keV and a current of 40 mA. The surface morphologies were investigated using atomic force

microscopy (AFM, SHIMADZU, SPM-9500J3) and field emission scanning electron microscopy (FESEM, JSM-6701F).

3. RESULTS AND DISCUSSION

To order to discuss the role of the ZnO seed layers in the growth of the ZnO NRs, the structural and morphological properties of seed layers with various annealing temperatures were determined using XRD and AFM measurements.

Figure 1 shows the XRD patterns of 20-nm-thick ZnO layers with various annealing temperatures. All the samples have a hexagonal wurtzite structure of ZnO (JCPDS card no. 36-1451) and are randomly oriented. Meanwhile, the intensities of the diffraction peaks corresponding to the (100), (002), and (101) orientations slightly increase with an increase in the annealing temperature. It was reported that the growth of NRs could be induced by the seed layer as nucleus centers on the surface of the substrate [16].

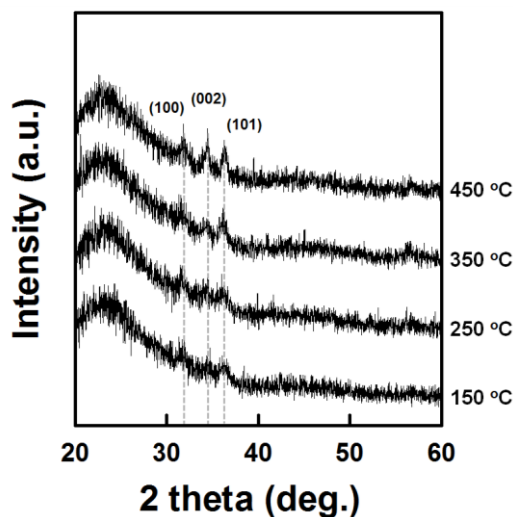


Figure 1. XRD patterns of 20-nm-thick ZnO layers with various annealing temperatures.

Figure 2 shows 2D AFM images of the ZnO seed layers and FESEM images of the ZnO NRs grown on seed layers with seed annealing temperatures from 150 °C to 450 °C. The growth time of the NRs was 3 h. From the AFM images, the ZnO particle size gradually increased with increasing annealing temperatures. This shows a good match with the XRD results (Fig. 1). The value of the RMS (room mean square) roughness slightly increased from 1.9 nm to 2.6 nm with increasing temperature from 150 °C to 350 °C, and decreased with further increases in the annealing temperature. It is noteworthy that the variation in the seed layer annealing temperature led to a significant change in the growth of the ZnO NRs. From cross-sectional FESEM images, the average length of the NRs increased from 100 nm to 380 nm with an increase in the seed annealing temperature from 150 °C to 350 °C and decreased with a further increase in the seed annealing temperature to 450 °C. This shows the same

tendency for the variation of the seed layer morphology as a function of the annealing temperature. This result is very consistent with the other report [17]. The growth rate of the ZnO NRs on the sputtered ZnO seed layer increased with increasing seed annealing temperature because of the improved crystallinity of the seed layer [17]. It was also reported that the length and alignment of ZnO nanowires (NWs) were strongly related to the thickness of the seed layers [18,19].

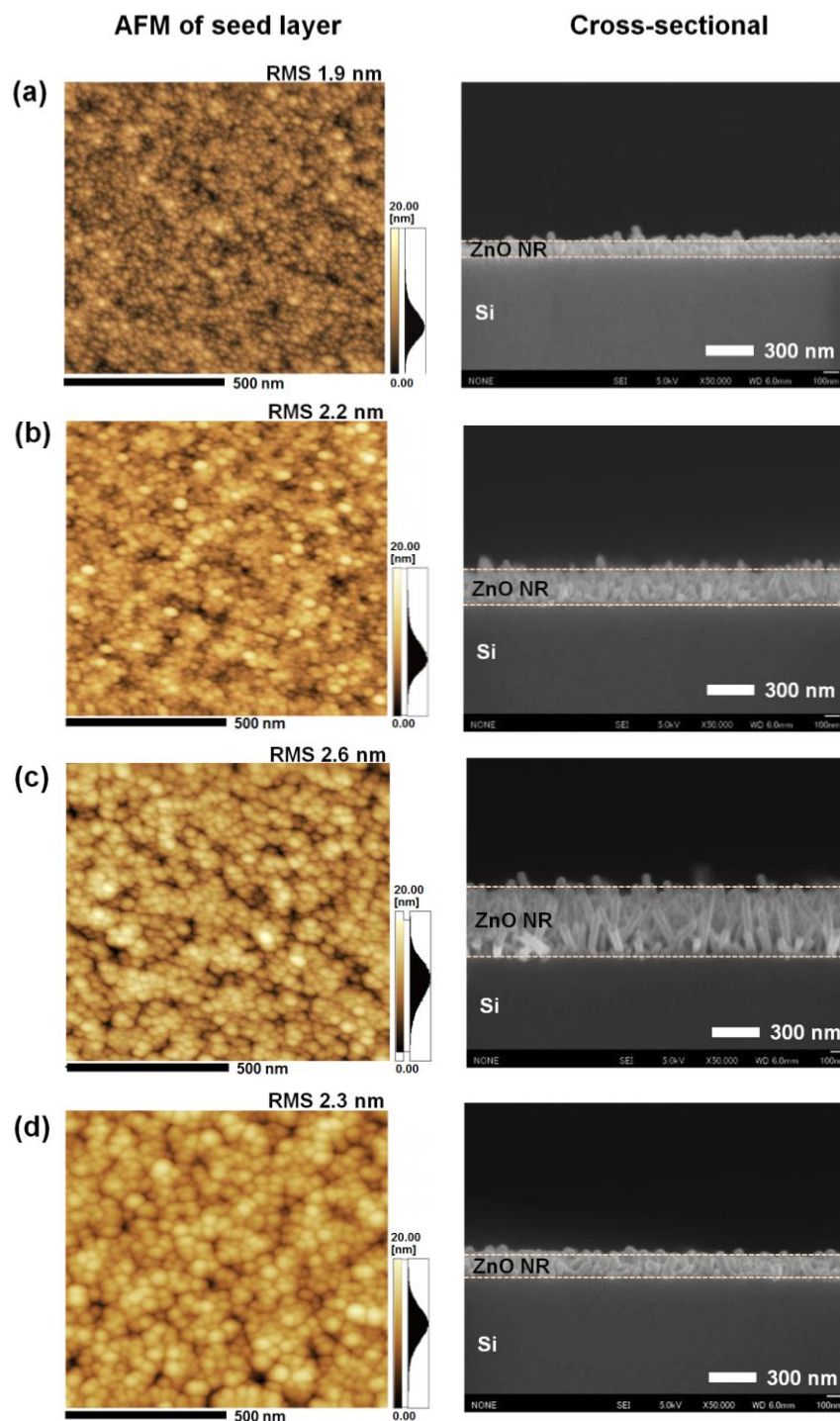


Figure 2. AFM images of seed layer and FESEM images of ZnO NRs grown on silicon substrates with different seed annealing temperatures: (a) 150 °C, (b) 250 °C, (c) 350 °C, and (d) 450 °C.

A thicker seed layer induced a well-aligned vertical growth of NWs. The seed annealing temperature is an important factor in the growth of NRs, along with the thickness. Wahid *et al.* reported the effect of the seed annealing temperature (100 °C–200 °C) on the growth of ZnO NRs. When the seed layer was annealed at a temperature greater than 150 °C, the homocentric bundling of ZnO NRs was observed on top of the vertical ZnO nanorods grown in the seed layer preparation on a 5-nm-thick Au-coated oxidized silicon (SiO₂) substrate because of the agglomeration of seed particles with temperature [20]. In our case, the structure of the NRs did not change with the seed annealing temperature.

To study the effect of the substrate material on the growth of the ZnO NRs, we examined the surface morphologies of the ZnO seed layers on the glass and FTO coated glass substrates. Figure 3 (a) shows the RMS roughness values of the ZnO seed layers with the seed annealing temperature on the silicon, glass, and FTO/glass substrates. Interestingly, the variation in the RMS roughness of the ZnO layer increases until a certain temperature (350 °C) and then decreases as a function of the annealing temperature regardless of the substrate material. At the same annealing temperature, the surface morphology is rougher in the order of the silicon, glass, and FTO coated glass. The surface morphologies of the bare substrate materials are shown in Fig. 3 (b). It should be noted that the nanostructures on the FTO substrate have a rougher surface morphology (RMS ~ 23.9 nm) than the silicon (RMS ~ 0.2 nm) and glass (RMS ~ 0.3 nm) bare substrates, which may be attributed to the original rough surface morphology of the ZnO layer on the FTO.

Figure 4 shows AFM images of the ZnO seed layers annealed at 350 °C on the silicon (a), glass (b), and FTO coated glass (c) substrates. The particle size of the seed layer is a critical parameter in determining the diameter of the ZnO NRs [21,22]. Because of the morphologies of the bare substrate materials (Fig. 3(b)), the value of the RMS roughness of the ZnO layer differs with the substrates.

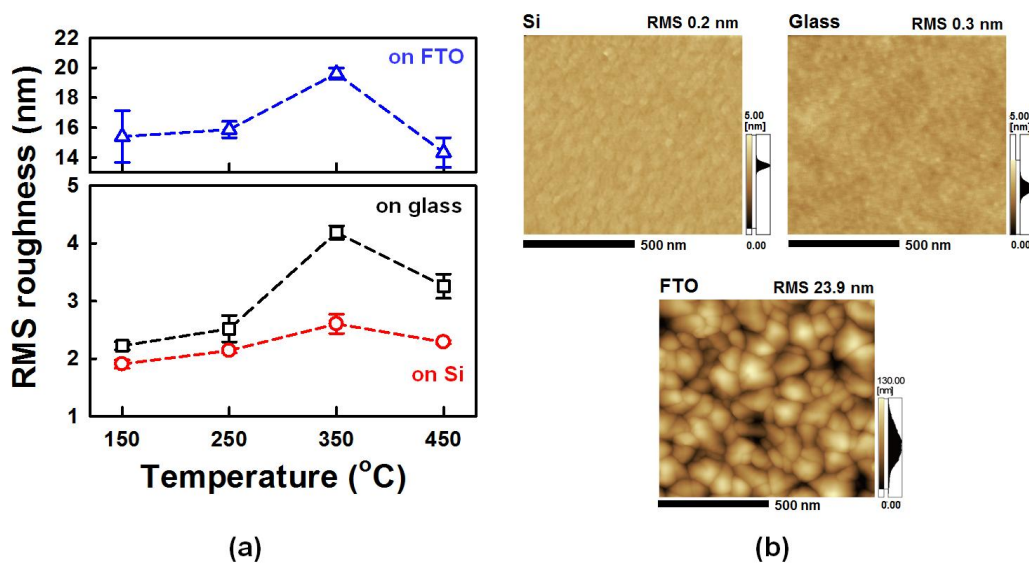


Figure 3. (a) RMS roughness values of ZnO seed layers prepared on various substrate materials with annealing temperature and (b) AFM images of bare silicon, glass, and FTO coated glass substrates.

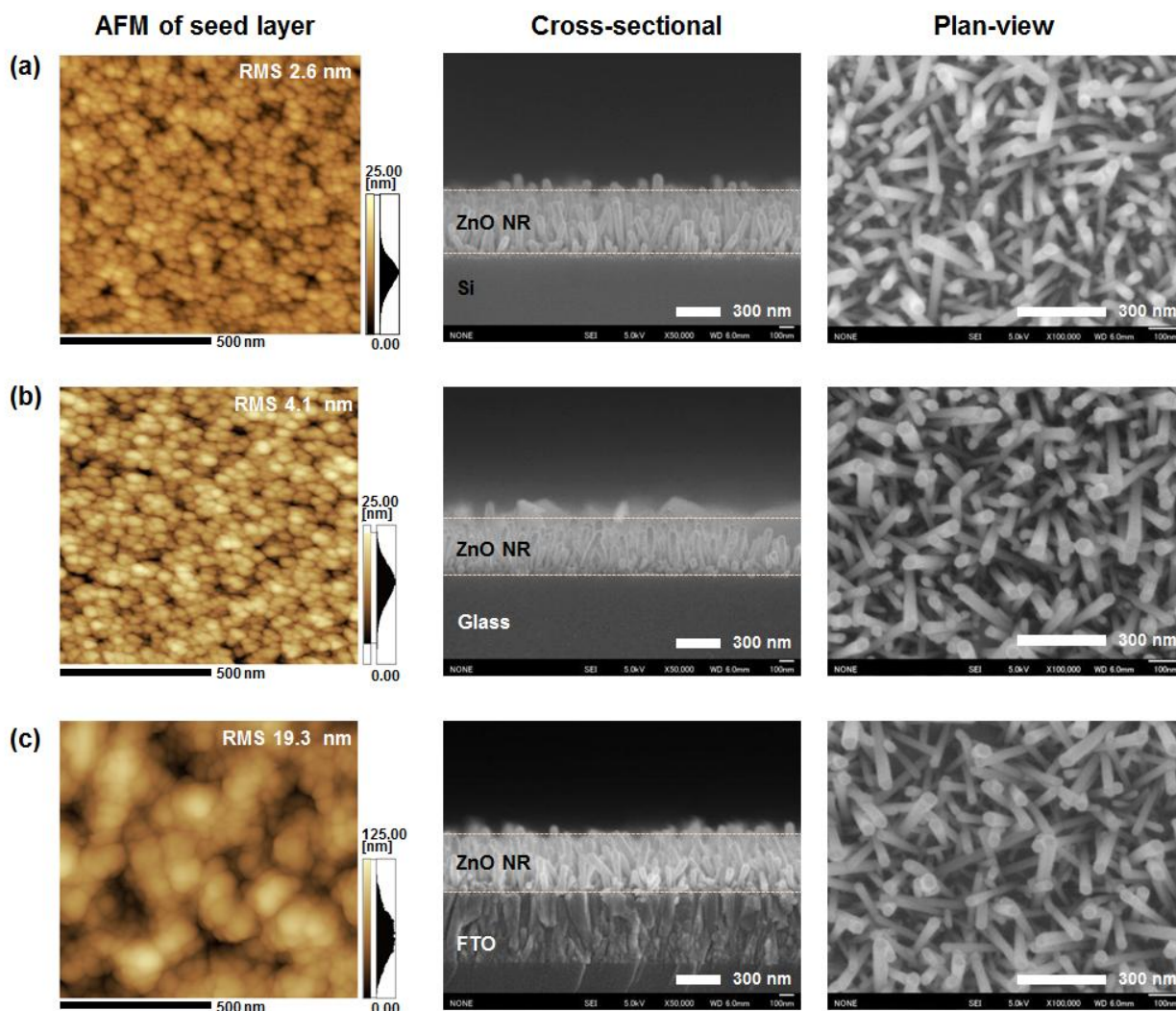


Figure 4. AFM images of seed layer annealed at 350 °C and FESEM images of ZnO NRs grown for 3 h on different substrate materials: (a) silicon, (b) glass, and (c) FTO/glass.

However, the particle size of the ZnO is approximately 40 nm, with no distinguishable difference between the substrate materials. This might be because of its thin film thickness. The crystalline size and crystallinity are strongly dependent on the film thickness [23,24]. From the FESEM images, it was found that the NRs grown on the seed layers prepared on the various substrate materials (silicon (a), glass (b), and FTO (c)) showed the similar growth behaviors. The average length, diameter, and density of the NRs were 380 nm, 40 ± 10 nm, and 270 ± 10 per μm^2 , respectively, with no obvious differences seen between the substrate materials.

Figure 5 shows FESEM images of the ZnO NR arrays grown on the silicon substrates with various growth times. The average length and density of the NRs with the growth time are plotted in Fig. 6 (a). The average length of the NRs increases from 1.0 μm to 1.9 μm with increasing growth time from 6 h to 12 h. From the FESEM images (d–f), the NRs possess a hexagonal surface and grew uniformly on the surface of the substrate. With increasing growth time, the self-attraction phenomenon is clearly observed [25–27], as shown in the inset images of Fig. 5 (d–f). During the growth process,

the tips of several NRs touch and/or cross each other, initially because of their slightly tilted growth and the piezoelectric properties of ZnO NRs, which lead to an increase in the diameter of the NRs and a decrease in their density with an increase in the growth time.

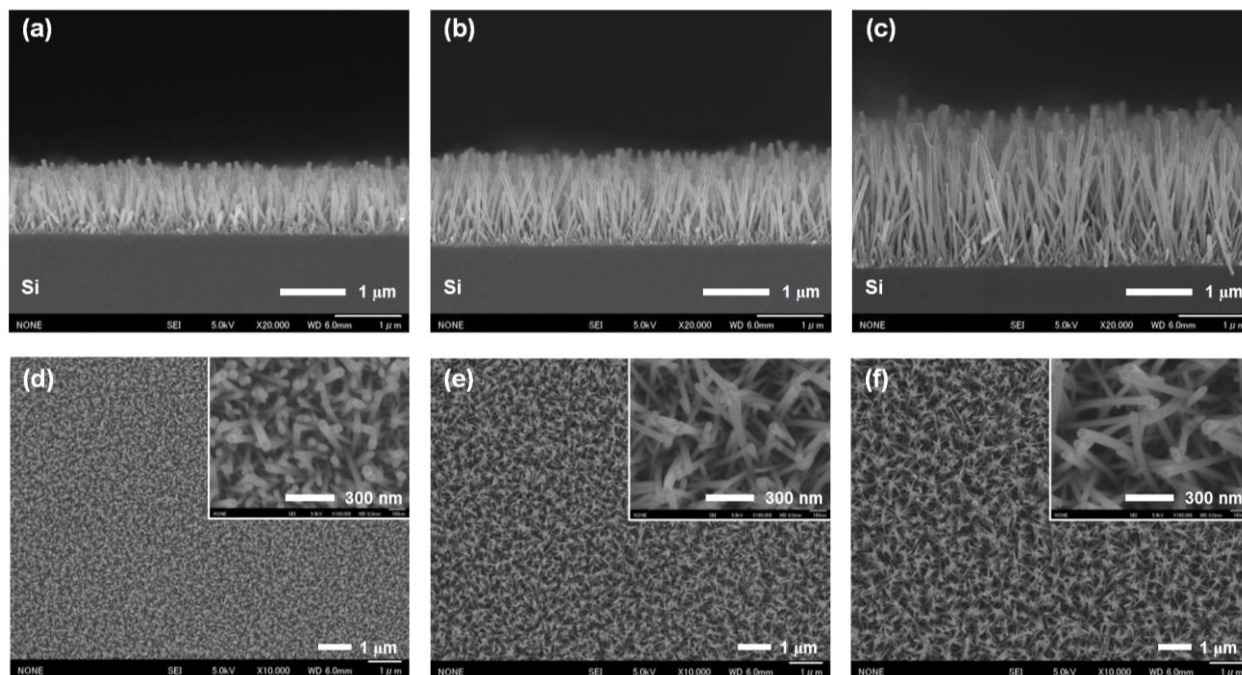


Figure 5. (a-c) Cross-sectional and (d-f) plan-view FESEM images of ZnO NRs grown on silicon substrates with various growth times: (a, d) 6 h, (b, e) 9 h, and (c, f) 12 h.

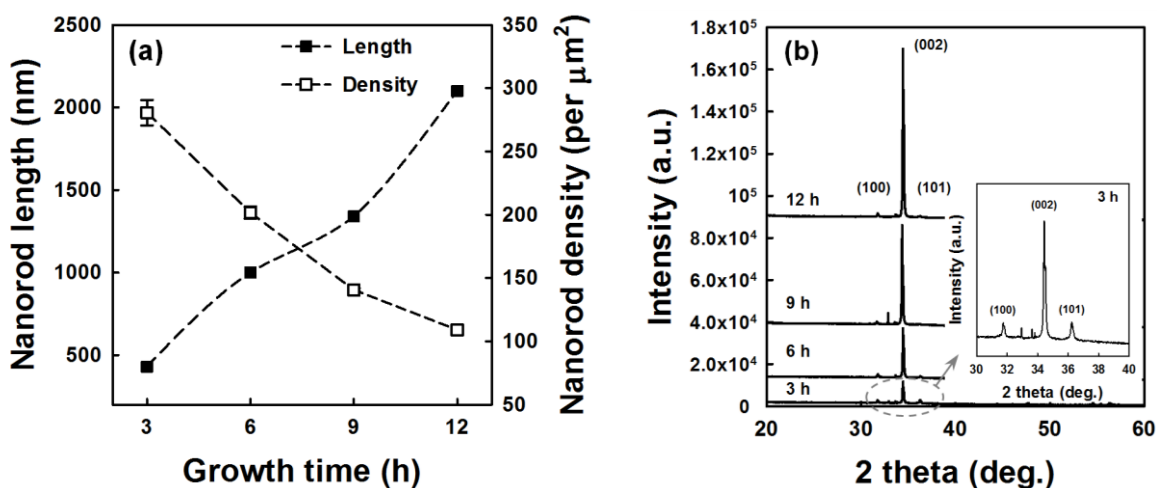


Figure 6. (a) Average length and density and (b) XRD patterns of ZnO NRs with various growth times. The inset figure is the XRD pattern of NRs grown for 3 h.

The XRD patterns of the ZnO NRs with growth times from 3 h to 12 h are shown in Fig. 6 (b). With increasing growth times, there is a significant increase in the intensity of the diffraction peak

corresponding to the (002) plane perpendicular to the substrate. Meanwhile, the weak diffraction peaks of (100) and (101) also appear, as shown in the inset figure, which is the XRD pattern of the NRs grown for 3 h. The relative intensity ratio of $i_{(002)}$, defined as $i_{(002)} = I_{(002)} / [I_{(100)} + I_{(002)} + I_{(101)}]$, of the NRs grown for 12 h is 0.95, which is significantly improved compared to that of ZnO NRs grown for 3 h ($i_{(002)} = 0.72$). During the self-attracting process, the NRs are dominantly grown to the (002) plane because of its lower surface free energy (1.6 J/m^2) compared to the (100) (3.4 J/m^2) and (101) (2.0 J/m^2) planes [15,28,29]. Therefore, it exhibits highly aligned c-axis oriented ZnO NRs with increasing growth times.

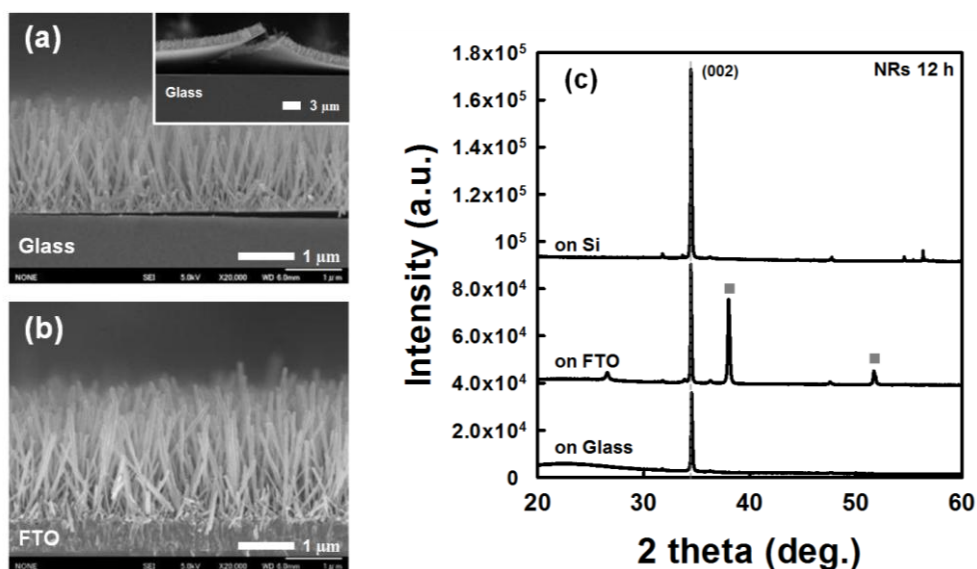


Figure 7. Cross-sectional FESEM images of ZnO NRs grown on (a) glass and (b) FTO/glass substrates, and (c) XRD patterns of ZnO NRs on various substrate materials (growth time of NRs is 12 h). The squares in (c) indicate the diffraction peaks corresponding to the FTO substrate.

Cross-sectional FESEM images of the ZnO NR arrays grown for 12 h on the glass and FTO coated glass substrates are shown in Fig. 7 (a) and (b), respectively. The average length and diameter of the NRs are $1.9 \mu\text{m}$ and $60 \pm 10 \text{ nm}$, respectively, which are less dependent on the substrate material. This indicates that the substrate material is not a vital parameter in relation to the length and diameter of the NRs grown at a fixed seed annealing temperature. The growth of well-aligned ZnO NRs on the FTO substrate provides great potential for optoelectric device applications [1,2,5]. Meanwhile, a clear difference was found in relation to the adhesion between the NRs and the substrate materials. Compared to the NRs grown on the silicon (Fig. 5 (c)) and FTO (Fig. 7 (b)) substrates, it shows poor adhesion between the NRs and the glass substrate. As shown in Fig. 7 (a) and its low-magnified view (inset of Fig. 7 (a)), the majority of the NRs peeled off and cracked, but a small portion was still attached to the glass substrate. It was reported that a silicon substrate gave a ZnO film with better crystallinity compared to a glass substrate [30]. This is very consistent with the following XRD results, as shown in Fig. 7 (c). All the NRs show good c-axis orientations perpendicular to the substrates, but

the intensity of the (002) diffraction peak increases in the order of the glass, FTO, and silicon. This indicates that the crystallinity of the NRs grown on the silicon substrate is better than the others. It was reported that the mismatch between the ZnO crystal structure and the silicon was less than the mismatch between the ZnO and glass [31]. The peak position of (002) for the NRs on the silicon and FTO substrates is 34.44° , whereas it shifts to a higher value (34.50°) in the case of the NRs grown on the glass substrate. This indicates a slight decrease in the c-axis value (5.1948 \AA) compared to that of the bulk ZnO (5.2066 \AA), implying that the NRs on the glass substrate suffer more tensile stress along the interface compared to those on the other substrates [32,33].

4. CONCLUSIONS

The ZnO seed layer conditions were critical parameters for the growth of ZnO NRs. The average length of the NRs increased until a certain seed annealing temperature and then slightly decreased with a further increase in temperature. The same tendency was seen for the seed layer morphology with increase in the annealing temperature. With the same particle size for the seed layer at a fixed annealing temperature, no obvious difference was seen in the NR growth rates for the various substrate materials (silicon, glass, FTO/glass). However, the NRs grown on the glass had tensile stress, which resulted in their peeling-off and cracking. The crystallinity of the NRs grown on the silicon was better than those grown on the other materials. During the NR growth process, the self-attracting NRs induced a highly c-axis orientation on the substrate.

ACKNOWLEDGEMENT

This work was supported by the Grant-in-Aid for Young Scientists (B) (24760245) from the Japan Society for the Promotion of Science (JSPS).

References

1. L.E. Greene, B.D. Yuhas, M. Law, D. Zitoun, and P. Yang, *Inorg. Chem.*, 45 (2006) 7535.
2. Q. Zhang, C.S. Dandeneau, X. Zhou, and G. Cao, *Adv. Mater.*, 21 (2009) 4087.
3. B. Kumar and S-W. Kim, *Nano Energy*, 1 (2012) 342.
4. S. Thiemann, M. Gruber, I. Lokteva, J. Hirschmann, M. Halik, and J. Zaumseil, *ACS Appl. Mater. Interfaces*, 5 (2013) 1656.
5. J.Y. Park, S-W. Choi, and S.S. Kim, *Nanoscale Res. Lett.*, 5 (2010) 353.
6. Y-M. Lee, C-M. Huang, H-W. Chen, and H-W. Yang, *Sensor. Actuat. A*, 189 (2013) 307.
7. L-W. Ji, S-M. Peng, J-S. Wu, W-S. Shih, C-Z. Wu, and I-T. Tang, *J. Phys. Chem. Solids*, 70 (2009) 1359.
8. Z.H. Ibupoto, K. Khun, M. Eriksson, M. AlSalhi, M. Atif, A. Ansari, and M. Willander, *Materials*, 6 (2013) 3584.
9. J.F. Muth, R.M. Kolbas, A.K. Sharma, S. Oktyabrsky, and J. Narayan, *J. Appl. Phys.*, 85 (1999) 7884.
10. Y. Natsume and H. Sakata, *Thin Solid Films*, 372 (2000) 30.
11. Y.H. Hwang, S-J. Seo, and B-S. Bae, *J. Mater. Res.*, 25 (2010) 695.

12. K.H. Kim, K. Utashiro, Z. Jin, Y. Abe, and M. Kawamura, *Int. J. Electrochem. Sci.*, 8 (2013) 5183.
13. D. Huang, F. Liao, S. Molesa, D. Redinger, and V. Subramanian, *J. Electrochem. Soc.*, 150 (2003) G412-G417.
14. D.H. Kim, H-J. Koo, J.S. Jur, M. Woodroof, B. Kalanyan, K. Lee, C.K. Devine, and G.N. Parsons, *Nanoscale*, 4 (2012) 4731-4738.
15. J. Lv, J. Zhu, K. Huang, F. Meng, X. Song, and Z. Sun, *Appl. Surf. Sci.*, 257 (2011) 7534.
16. Q. Huang, L. Fang, X. Chen, and M. Saleem, *J. Alloys Compd.*, 509 (2011) 9456.
17. C. Li, G. Fang, J. Li, L. Ai, B. Dong, and X. Zhao, *J. Phys. Chem. C*, 112 (2008) 990.
18. N. Fujimura, T. Nishihara, S. Goto, J. Xu, and T. Ito, *J. Crystal Growth*, 130 (1993) 269.
19. C.Y. Kung, S.L. Young, M.C. Kao, H.Z. Chen, J.H. Lin, H.H. Lin, L. Horng, and Y.T. Shih, *IEEE 5th International Nanoelectronics Conference (INEC)*, 2013, 417.
20. K.A. Wahid, W.Y. Lee, H.W. Lee, A.S. The, D.C.S. Bien, and I.A. Azid, *Appl. Surf. Sci.*, 283 (2013) 629.
21. W-Y. Wu, C-C. Yeh, and J-M. Ting, *J. Am. Ceram. Soc.*, 92 (2009) 2718.
22. H. Ghayour, H.R. Rezaie, Sh. Mirdamadi, and A.A. Nourbakhsh, *Vacuum*, 86 (2011) 101.
23. N. Kakati, S.H. Jee, S.H. Kim, J.Y. Oh, and Y.S. Yoon, *Thin Solid Films*, 519 (2010) 494.
24. J.Y.W. Seto, *J. Appl. Phys.*, 46 (1975) 5247.
25. X. Han, G. Wang, L. Zhou, and J.G. Hou, *Chem. Commun.*, (2006) 212.
26. J. Liu, S. Xie, Y. Chen, X. Wang, H. Cheng, F. Liu, and J. Yang, *Nanoscale Res. Lett.*, 6 (2011) 619.
27. S. Lin, H. Hu, W. Zheng, Y. Qu, and F. Lai, *Nanoscale Res. Lett.*, 8 (2013) 158.
28. P. Singh, A. Kumar, Deepak, and D. Kaur, *J. Crystal Growth*, 306 (2007) 303.
29. S. Liang and X. Bi, *J. Appl. Phys.*, 104 (2008) 113533.
30. C. Periasamy, R. Prakash, and P. Chakrabarti, *J. Mater. Sci: Mater Electron*, 21 (2010) 309.
31. V. Ghafouri, M. Shariati, and A. Ebrahimzad, *Scientia Iranica F*, 19 (2012) 934.
32. Y.C. Liu, H.Y. Xu, R. Mu, D.O. Henderson, Y.M. Lu, J.Y. Zhang, D.Z. Shen, X.W. Fan, and C.W. White, *Appl. Phys. Lett.*, 83 (2003) 1210.
33. B.L. Zhu, X.Z. Zhao, F.H. Su, G.H. Li, X.G. Wu, J. Wu, and R. Wu, *Vacuum*, 84 (2010) 1280.